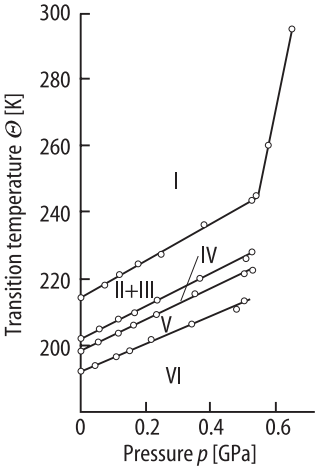

Fig. 22A-2-001. $TlInS_2$. Θ vs. p [88All].

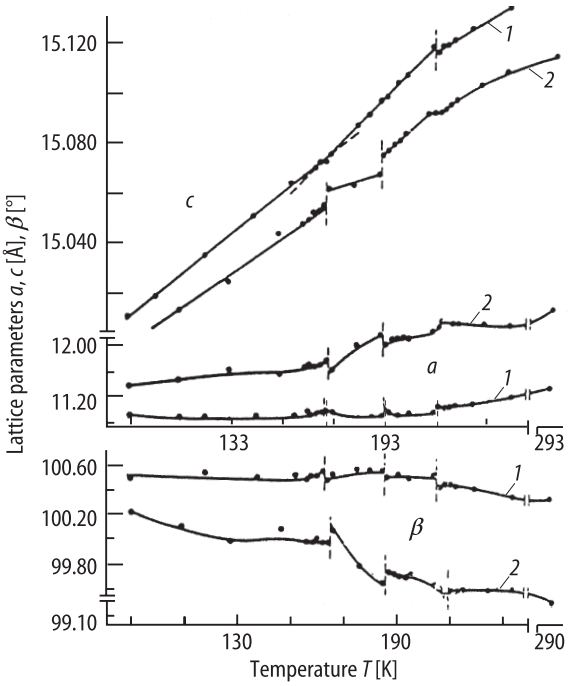

Fig. 22A-2-002. $TlInS_2$ (*1*), $Tl_{0.98}Cu_{0.02}InS_2$ (*2*). a, c, β vs. T [89Mal].

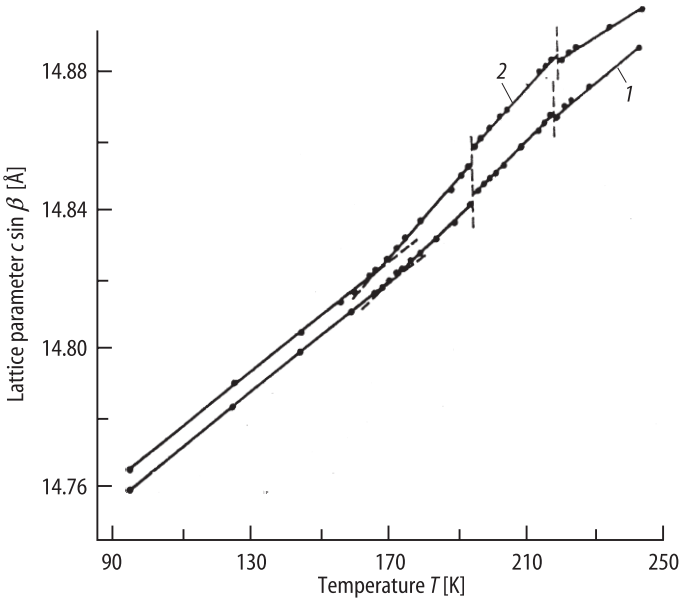

Fig. 22A-2-003. $TlInS_2$ (*1*), $Tl_{0.98}Cu_{0.02}InS_2$ (*2*). $c \sin \beta$ vs. T [89Mal].

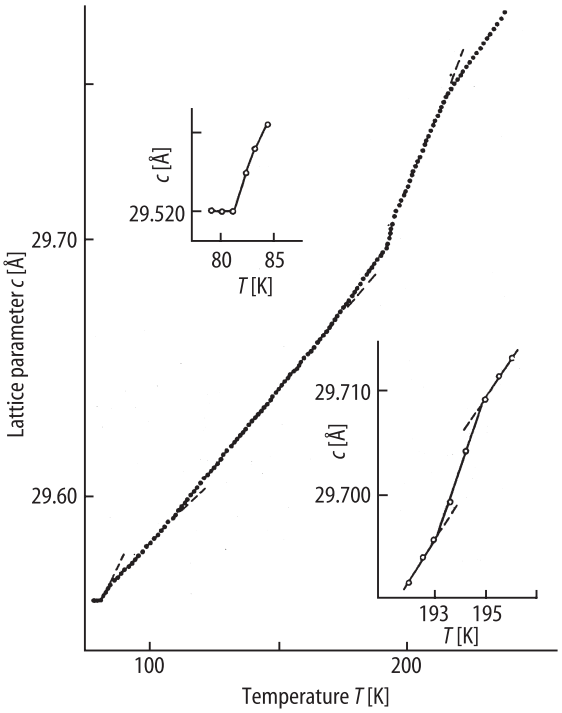

Fig. 22A-2-004. $TlInS_2$. c vs. T [89Ply].

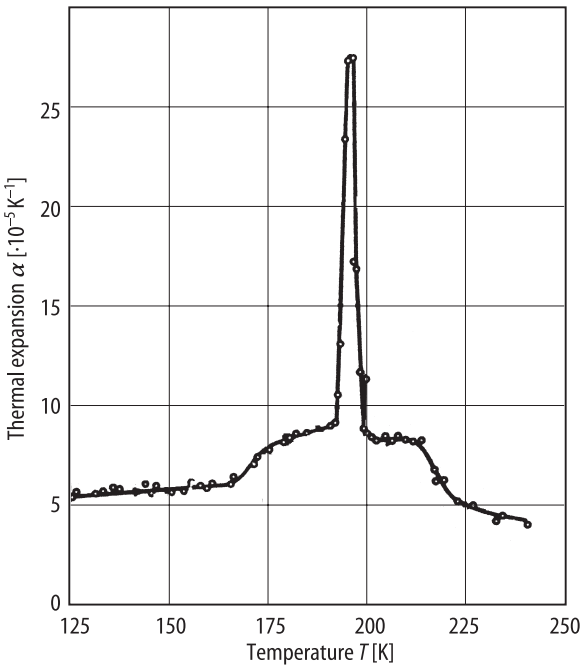

Fig. 22A-2-005. $TlInS_2$. α vs. T [84Vak]. α: thermal expansion coefficient.

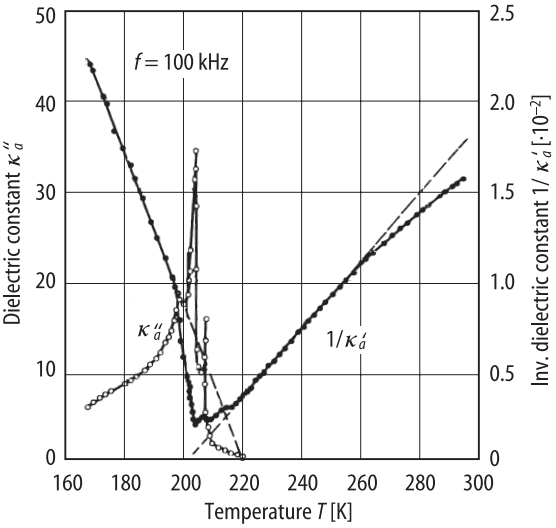

Fig. 22A-2-006. $TlInS_2$. $1/\kappa_a'$, κ_a'' vs. T [84Ali].

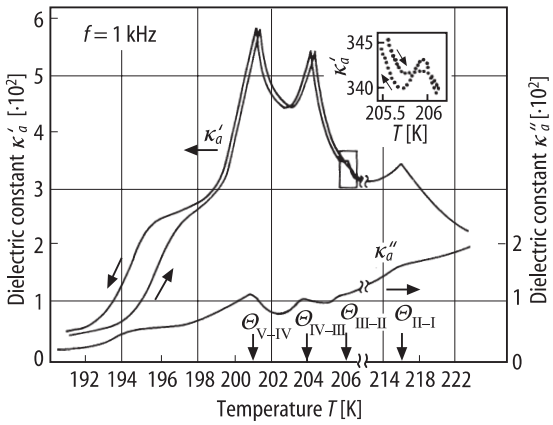

Fig. 22A-2-007. $TlInS_2$. κ'_a, κ''_a vs. T [95All].

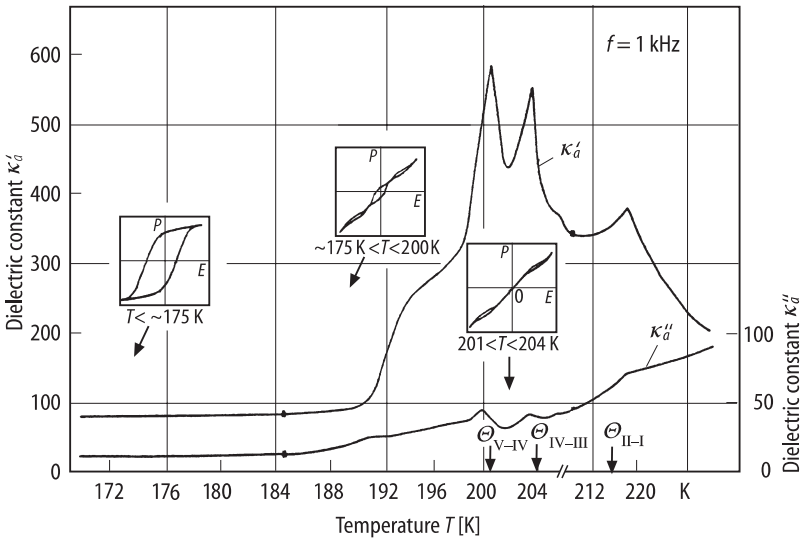

Fig. 22A-2-008. $TlInS_2$. κ'_a, κ''_a vs. T [92Sal]. Inserts: shapes of hysteresis loops.

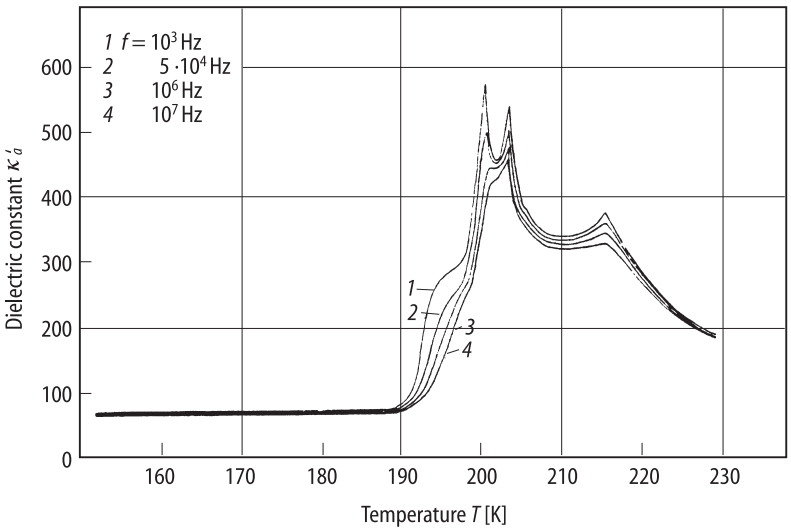

Fig. 22A-2-009. $TlInS_2$. κ'_a vs. T [92Sal]. Parameter: f.

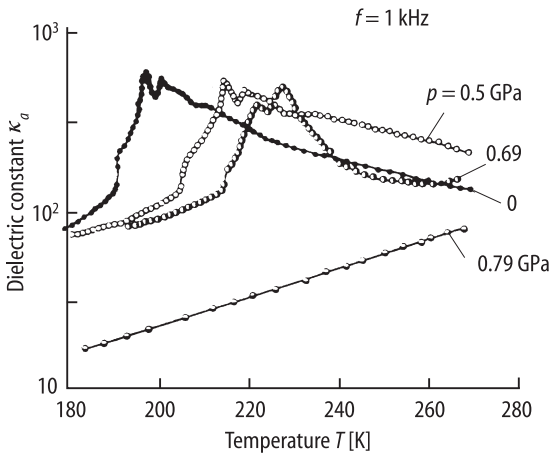

Fig. 22A-2-010. $TlInS_2$. κ_a vs. T [88All]. Parameter: p.

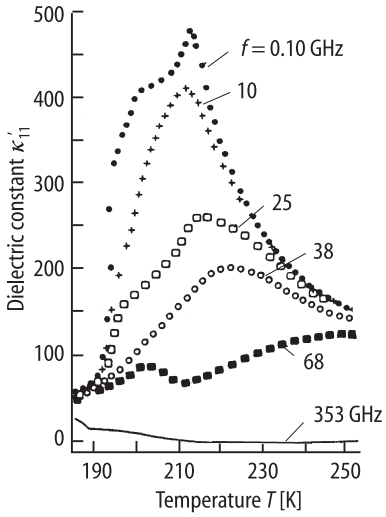

Fig. 22A-2-011. $TlInS_2$. κ'_{11} vs. T [88Ban]. Parameter: f = 0.10 ... 353 GHz [83Vol].

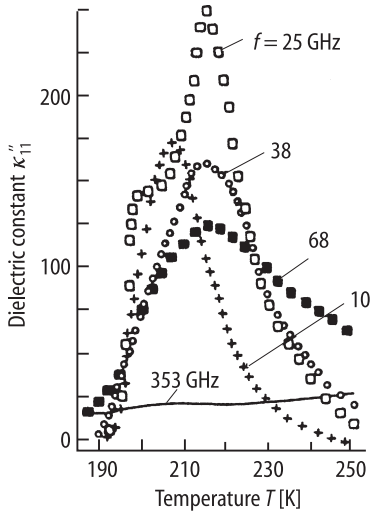

Fig. 22A-2-012. $TlInS_2$. κ''_{11} vs. T [88Ban]. Parameter: f = 25 ... 353 GHz [83Vol].

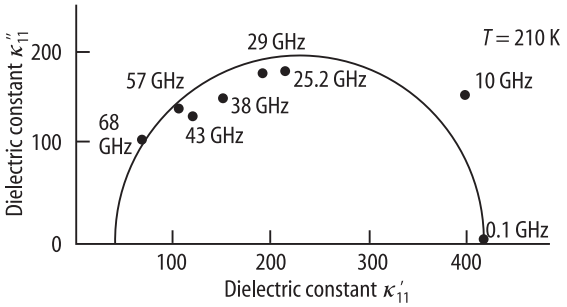

Fig. 22A-2-013. $TlInS_2$. Cole-Cole plot of complex dielectric constant at T = 210 K [88Ban].

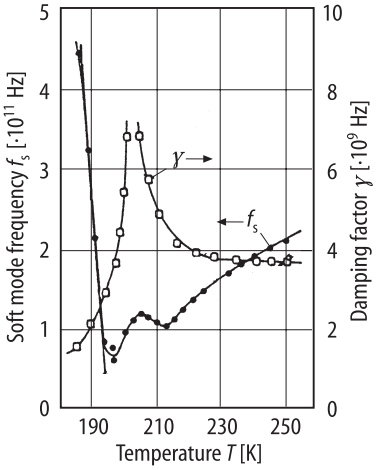

Fig. 22A-2-014. $TlInS_2$. f_s, γ vs. T [88Ban]. f_s: soft mode frequency, γ: damping factor.

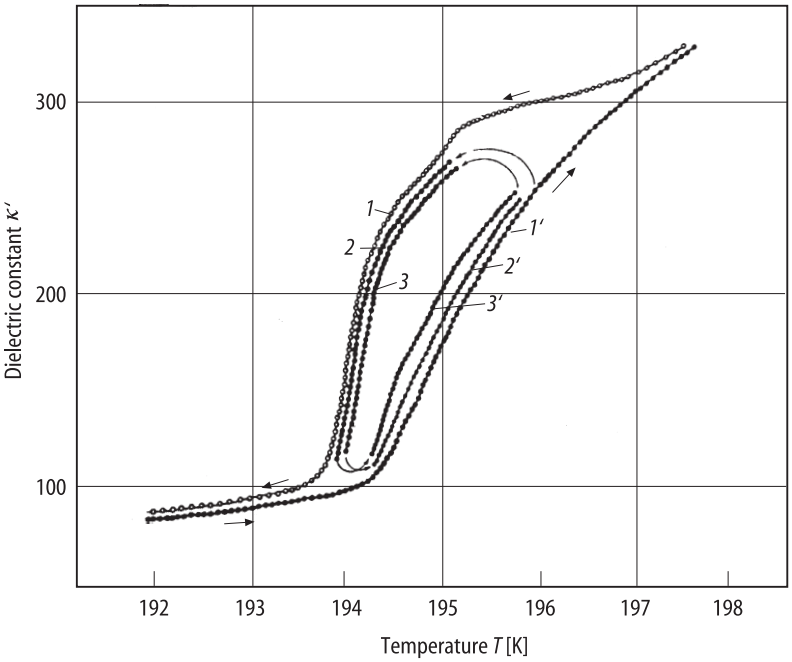

Fig. 22A-2-015. $TlInS_2$. Thermal hysteresis in κ' vs. T relationship [92Sal]. *1*, *2*, *3*: cooling; *1′*, *2′*, *3′*: heating.

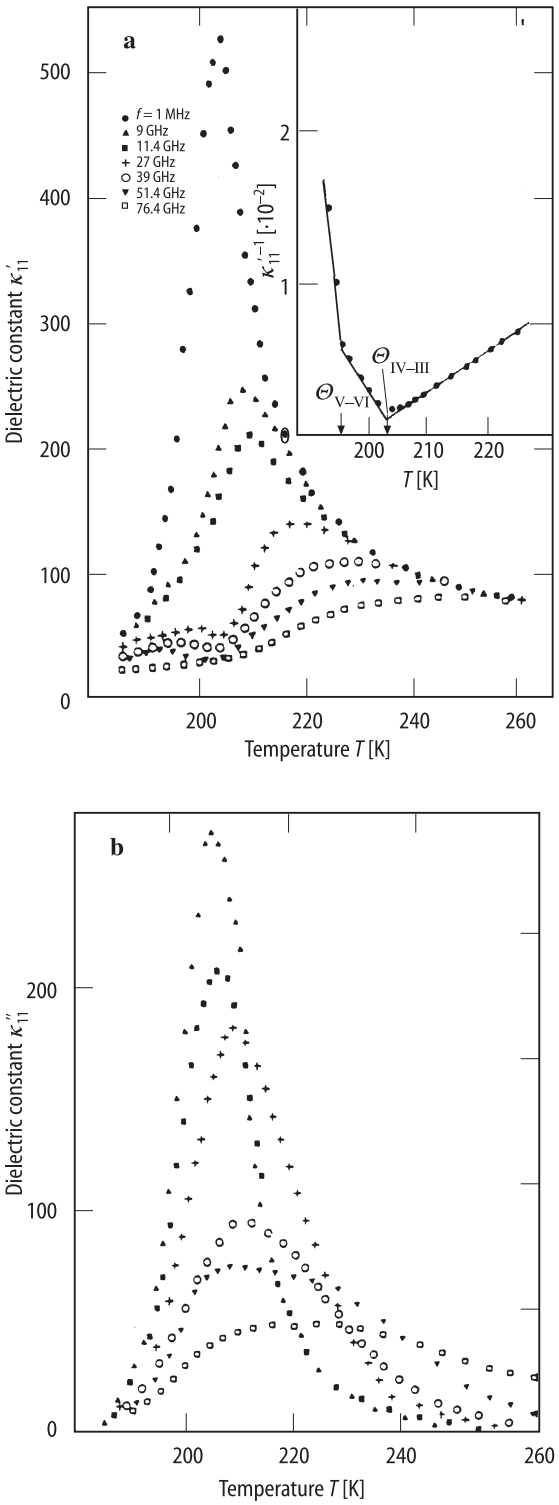

Fig. 22A-2-016. $TlInS_2$ with 1 % Fe admixture. (**a**) κ'_{11} vs. T, (**b**) κ''_{11} vs. T [90Ban]. Parameter: f. Insert in (**a**): $1/\kappa'_{11}$ vs. T at f = 1 MHz.

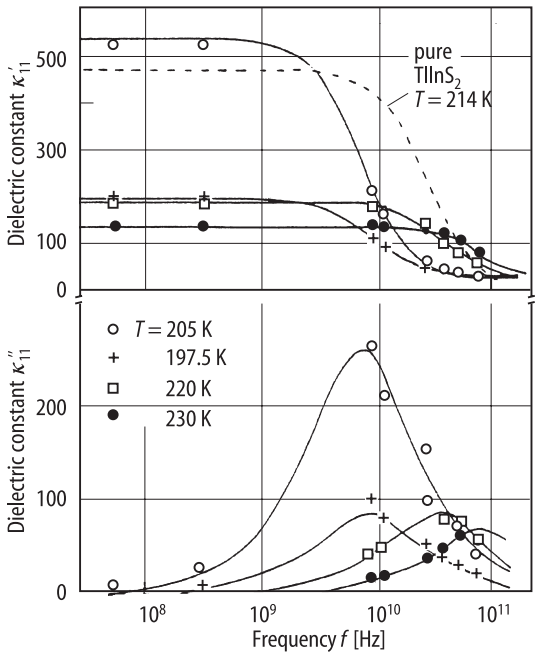

Fig. 22A-2-017. $TlInS_2$ with 1 % Fe admixture. κ'_{11}, κ''_{11} vs. f [90Ban]. Parameter: T. Dashed line: pure $TlInS_2$ at 214 K [88Ban].

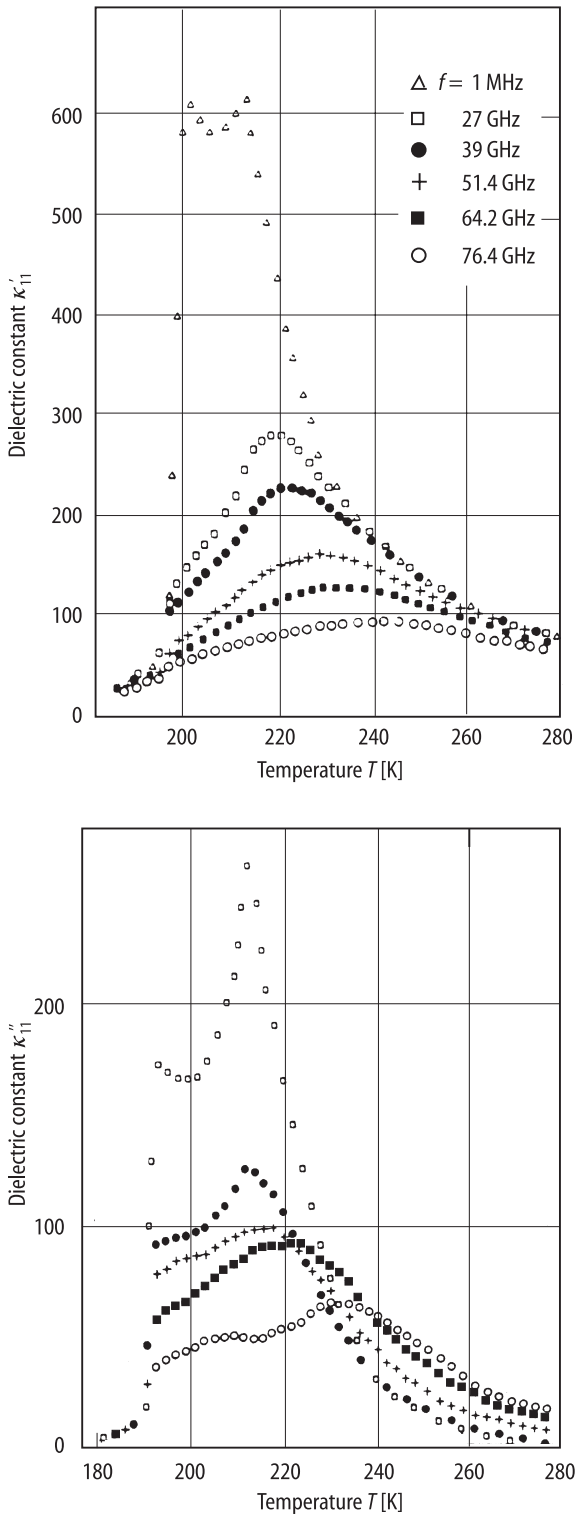

Fig. 22A-2-018. $TlInS_2$ with 1.5 % Cu admixture. κ'_{11}, κ''_{11} vs. T [90Ban]. Parameter: f.

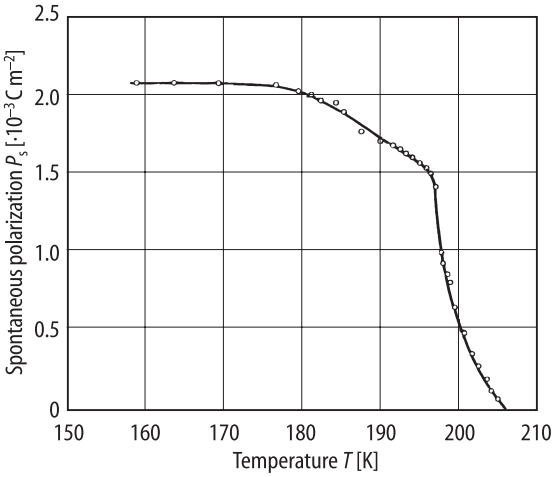

Fig. 22A-2-019. $TlInS_2$. P_s vs. T [84Ali].

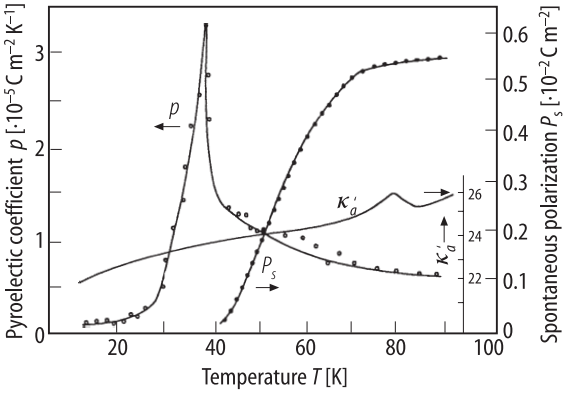

Fig. 22A-2-020. $TlInS_2$. κ'_a, p, P_s vs. T below 100 K [95All]. p: pyroelectric coefficient.

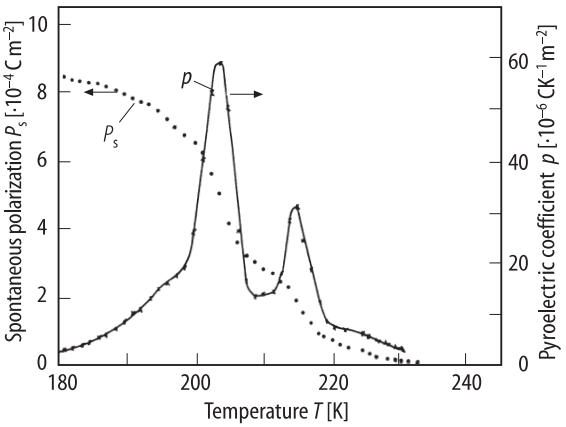

Fig. 22A-2-021. $TlInS_2$. P_s, p vs. T above 180 K [88All]. p: pyroelectric coefficient.

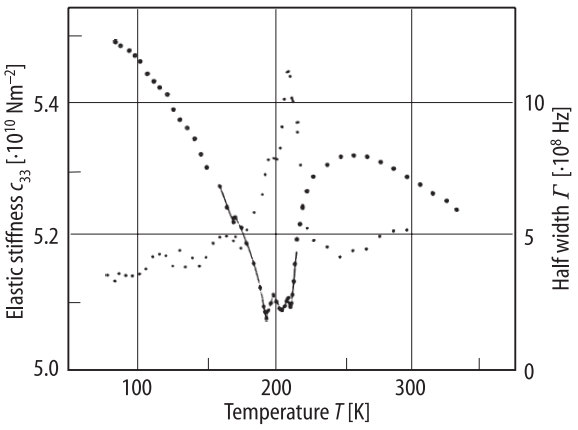

Fig. 22A-2-022. $TlInS_2$. c_{33}, Γ vs. T [88Lai].

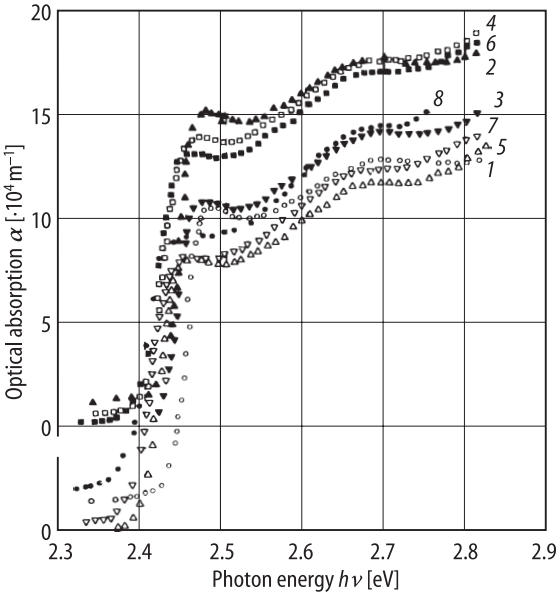

Fig. 22A-2-023. $TlInS_2$. α vs. $h\nu$ [86Bak]. α: optical absorption coefficient. Parameter: T. Curve *1*: 174 K, *2*: 183 K, *3*: 189 K, *4*: 196 K, *5*: 200 K, *6*: 209 K, *7*: 220 K, *8*: 240 K.

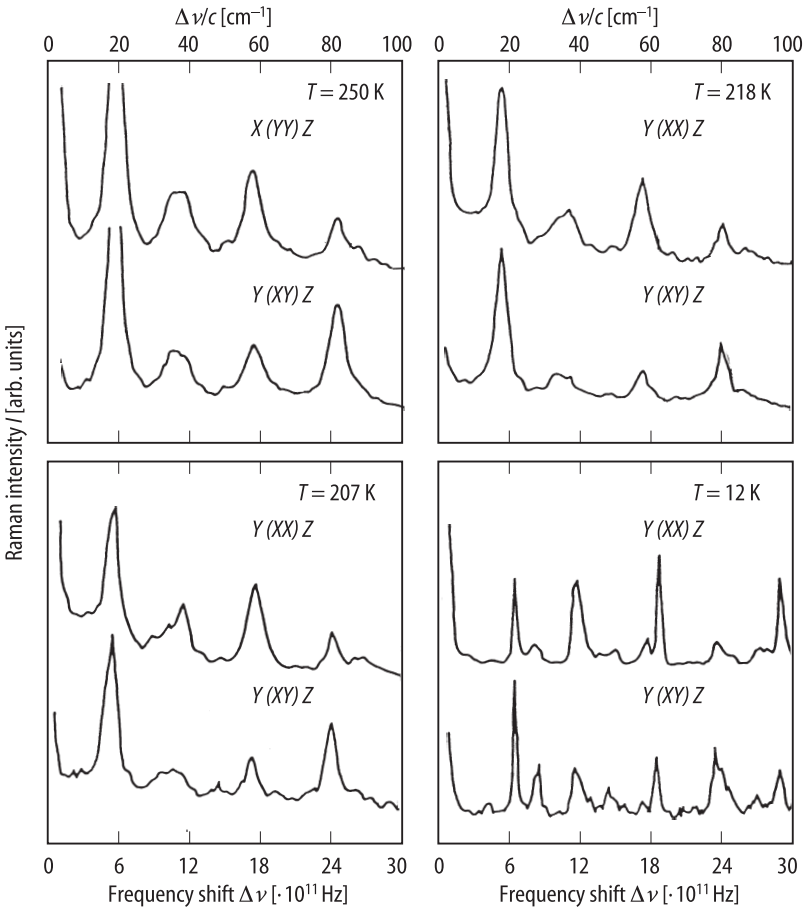

Fig. 22A-2-024. $TlInS_2$. I vs. $\Delta\nu$ [89All]. I: Raman scattering intensity of $X(YY)Z$, $Y(XX)Z$ and $Y(XY)Z$ geometries. Parameter: T.

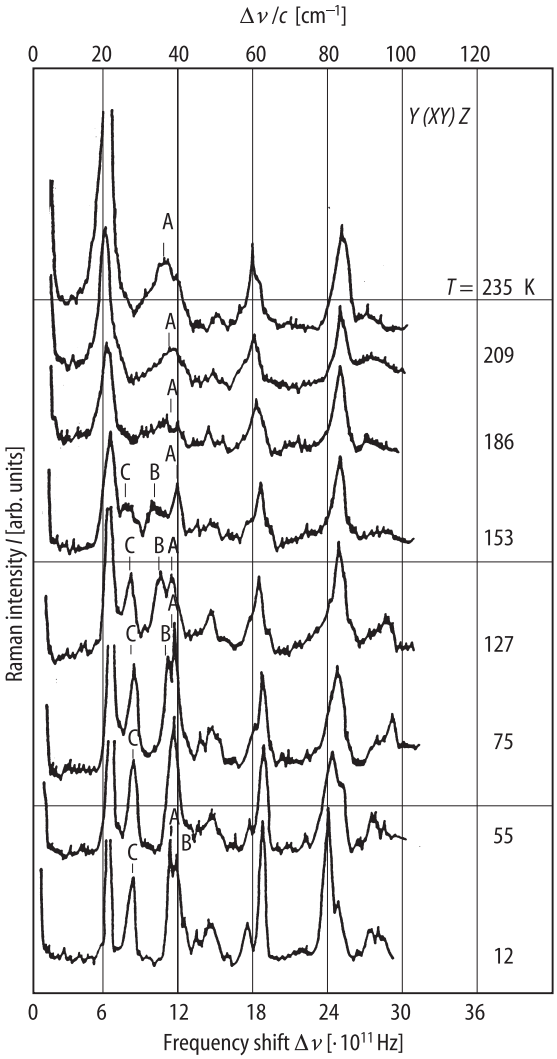

Fig. 22A-2-025. $TlInS_2$. *I* vs. $\Delta\nu$ [89All]. *I*: Raman scattering intensity of *Y*(*XY*)*Z* geometry. $\Delta\nu$: Raman frequency shift. Parameter: *T*.

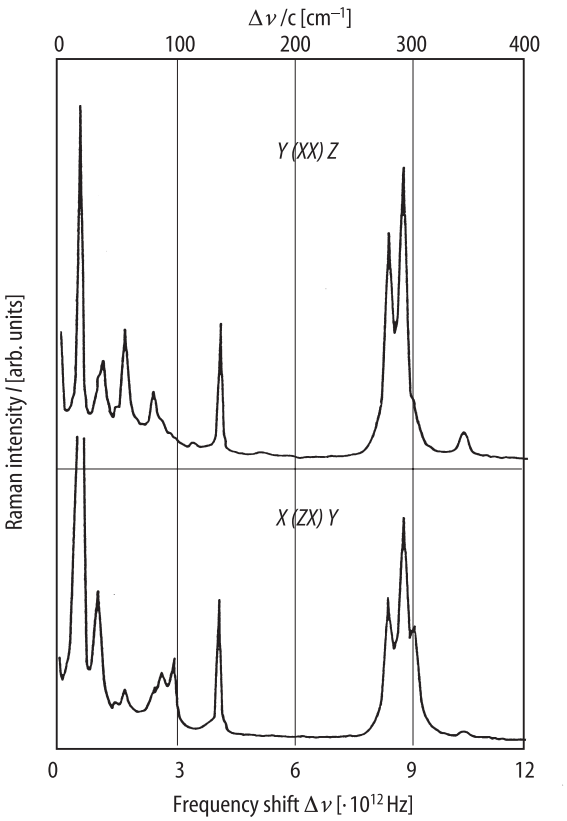

Fig. 22A-2-026. $TlInS_2$. I vs. $\Delta\nu$ [89All]. I: Raman scattering intensity of $Y(XX)Z$ and $X(ZX)Y$ geometries. $\Delta\nu$: Raman frequency shift.

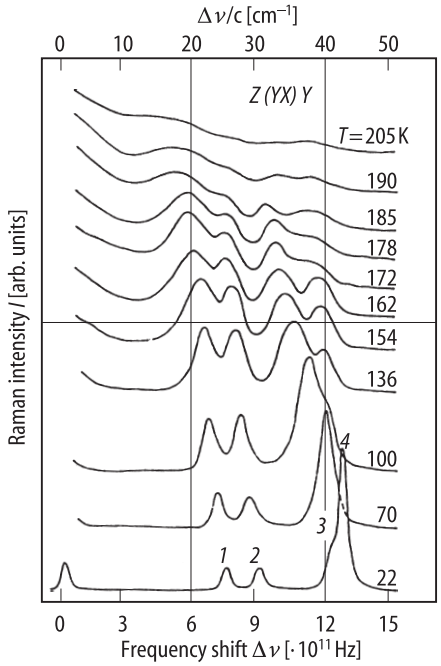

Fig. 22A-2-027. $TlInS_2$. I vs. $\Delta\nu$ [89All]. $\Delta\nu$: Raman frequency shift. I: Raman scattering intensity of $Z(YX)Y$ geometry. Parameter: T.

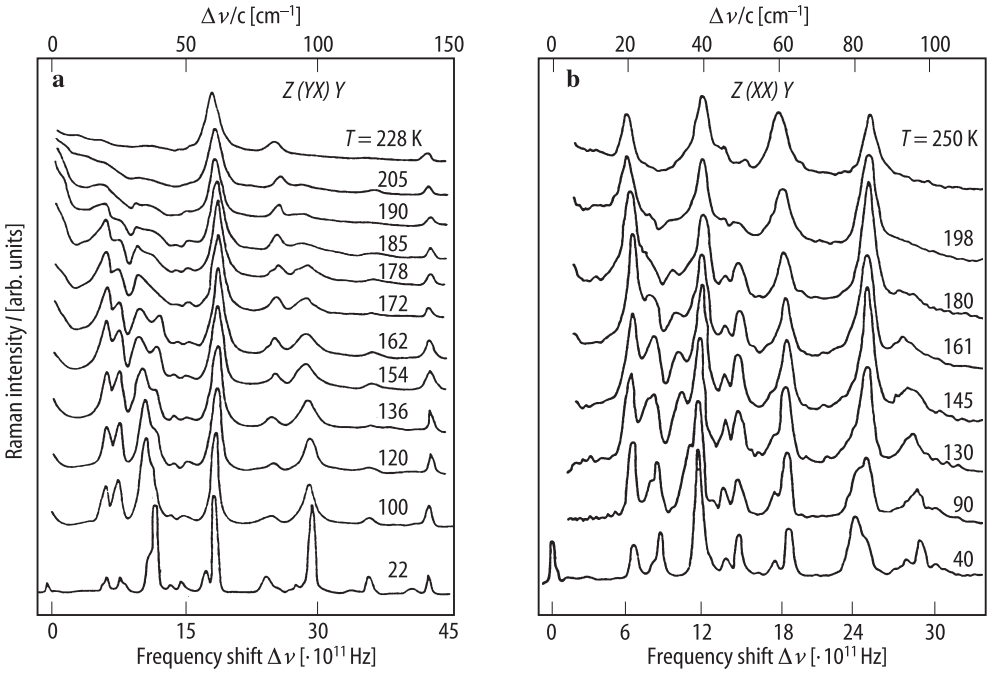

Fig. 22A-2-028. $TlInS_2$. I vs. $\Delta\nu$ [89Bur]. I: Raman scattering intensity of (**a**) $Z(YX)Y$ and (**b**) $Z(XX)Y$ geometries. Parameter: T.

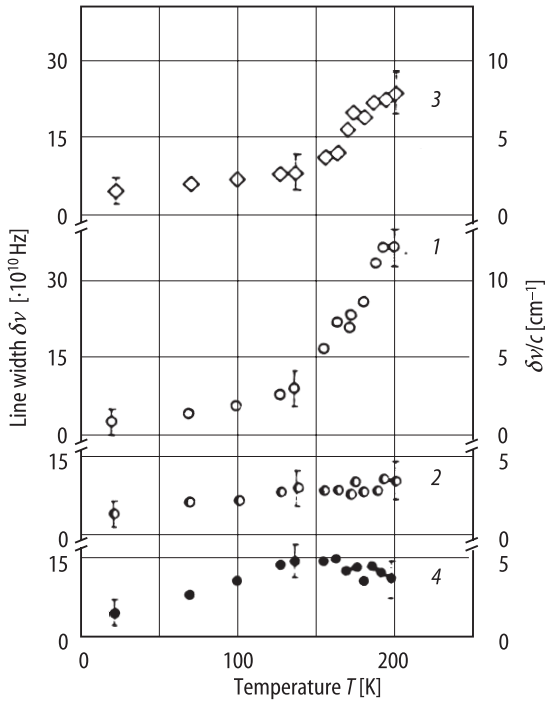

Fig. 22A-2-029. $TlInS_2$. $\delta\nu$ vs. T [89Bur]. $\delta\nu$: linewidth of Raman line.

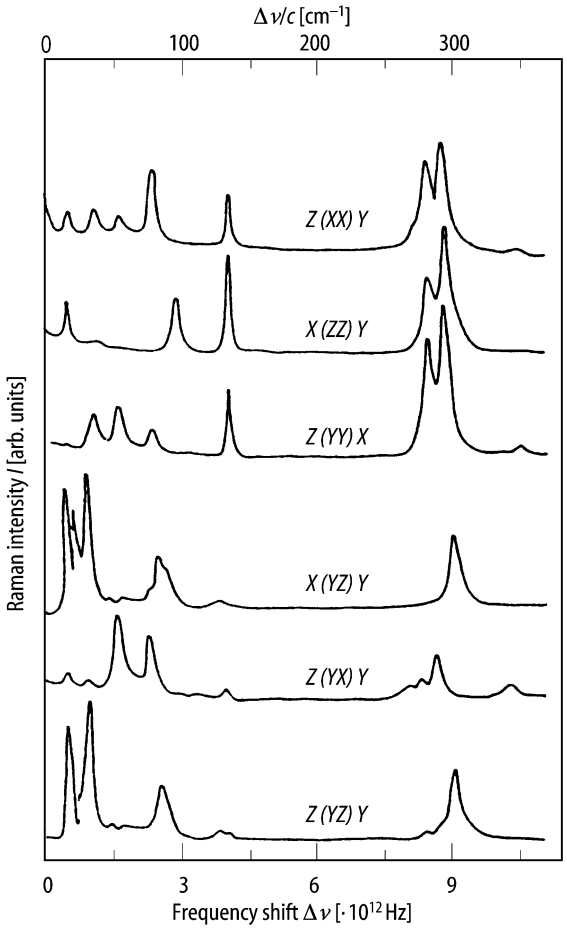

Fig. 22A-2-030. $TlInS_2$. I vs. $\Delta\nu$ [89Bur]. $\Delta\nu$: Raman frequency shift at room temperature. I: Raman scattering intensity.

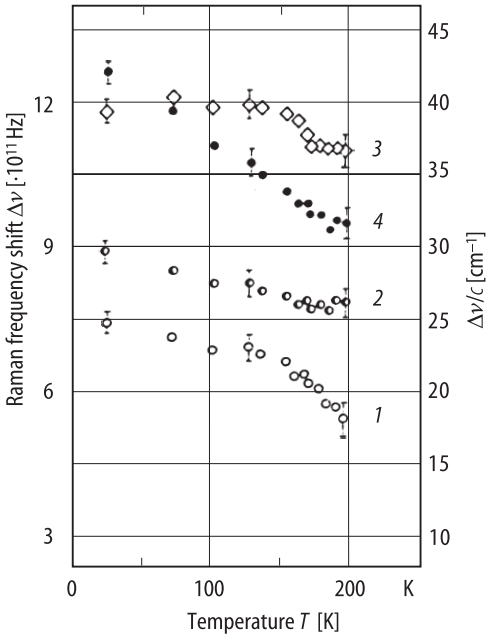

Fig. 22A-2-031. $TlInS_2$. $\Delta\nu$ vs. T [89Bur]. $\Delta\nu$: Raman scattering frequency shift. Parameter: peak numbers.

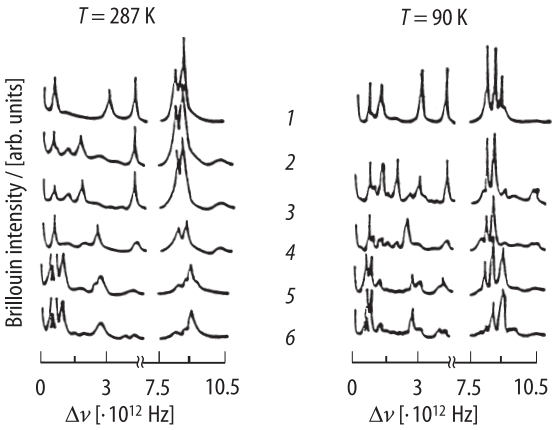

Fig. 22A-2-032. $TlInS_2$. I vs. $\Delta\nu$ [89Dur]. I: Brillouin scattering intensity of the LA mode. Parameter: scattering geometry, *1*: $Y(ZZ)X$, *2*: $Z(YY)X$, *3*: $Z(XX)Y$, *4*: $Y(XY)Z$, *5*: $Z(YZ)X$, *6*: $Z(XY)Y$.